Neuron
Article

Drosophila Neuroligin 1 Promotes Growth and Postsynaptic Differentiation at Glutamatergic Neuromuscular Junctions

Daniel Banovic,[1,6] Omid Khorramshahi,[2,6] David Owald,[2,4] Carolin Wichmann,[2,3] Tamara Riedt,[1,5] Wernher Fouquet,[2] Rui Tian,[2] Stephan J. Sigrist,[2,*] and Hermann Aberle[1,*]
[1]University of Münster, Institute for Neurobiology, Badestrasse 9, 48149 Münster, Germany
[2]Freie Universität Berlin, Institute for Biology/Genetics, Takustrasse 6, 14195 Berlin, Germany
[3]European Neuroscience Institute Göttingen, Grisebachstrasse 5, 37077 Göttingen, Germany
[4]Cluster of Excellence NeuroCure, Charite, Chariteplatz 1, 10117 Berlin, Germany
[5]Present address: University of Bonn, Department of Hematology/Oncology, Medical Center III, Wilhelmstrasse 35-37, 53111 Bonn, Germany
[6]These authors contributed equally to this work
*Correspondence: aberleh@uni-muenster.de (H.A.), stephan.sigrist@fu-berlin.de (S.J.S.)
DOI 10.1016/j.neuron.2010.05.020

SUMMARY

Precise apposition of presynaptic and postsynaptic domains is a fundamental property of all neuronal circuits. Experiments in vitro suggest that Neuroligins and Neurexins function as key regulatory proteins in this process. In a genetic screen, we recovered several mutant alleles of *Drosophila neuroligin 1* (*dnlg1*) that cause a severe reduction in bouton numbers at neuromuscular junctions (NMJs). In accord with reduced synapse numbers, these NMJs show reduced synaptic transmission. Moreover, lack of postsynaptic DNlg1 leads to deficits in the accumulation of postsynaptic glutamate receptors, scaffold proteins, and subsynaptic membranes, while increased DNlg1 triggers ectopic postsynaptic differentiation via its cytoplasmic domain. DNlg1 forms discrete clusters adjacent to postsynaptic densities. Formation of these clusters depends on presynaptic *Drosophila* Neurexin (DNrx). However, DNrx binding is not an absolute requirement for DNlg1 function. Instead, other signaling components are likely involved in DNlg1 transsynaptic functions, with essential interactions organized by the DNlg1 extracellular domain but also by the cytoplasmic domain.

INTRODUCTION

Synapses are specialized membrane contacts between presynaptic and postsynaptic cell compartments that are connected by cell-cell adhesion proteins, which regulate the assembly and maturation of synapses (Yamagata et al., 2003; Washbourne et al., 2004). Different classes of synaptic adhesion proteins have been identified, including members of the immunoglobulin superfamily, Eph/Ephrins, Cadherins, and the Neurexin/Neuroligin families (Dalva et al., 2007; Takeichi, 2007). A typical transsynaptic complex is formed by the heterophilic interaction of presynaptic Neurexins (Nrxs) and postsynaptic Neuroligins (Nlgs) (Dean and Dresbach, 2006). Nlgs are encoded by four independent genes in rodents and five genes in humans (Ichtchenko et al., 1995; Lisé and El-Husseini, 2006). Nlgs possess a catalytically inactive acetylcholinesterase-like domain, which interacts with presynaptic Nrxs (Ichtchenko et al., 1996; Araç et al., 2007; Fabrichny et al., 2007). Both Nrxs and Nlgs contain C-terminal, intracellular PDZ-domain-binding motifs believed to recruit scaffolding proteins for organization of either the presynaptic release machinery or the postsynaptic neurotransmitter receptors (Ushkaryov et al., 1992; Missler et al., 2003; Dean and Dresbach, 2006). Therefore, the interaction of Nrxs with Nlgs has the potential to assemble a large transsynaptic complex that mediates the precise apposition of presynaptic and postsynaptic membranes.

Nlgs localize to postsynaptic regions and, when expressed in nonneuronal cells, induce cocultured neurons to form presynaptic specializations onto the nonneuronal cell (Song et al., 1999; Scheiffele et al., 2000). In support for a central role in the formation of synaptic contacts, overexpression of Nlgs in cultured neurons increases not only the number and density of synapses, but also synaptic function (Chih et al., 2005; Levinson et al., 2005; Sara et al., 2005; Chubykin et al., 2007). Conversely, knockdown of Nlgs by RNA interference (RNAi) leads to a reduction of synapse numbers (Chih et al., 2005), suggesting a role for Nlgs in synapse formation, stability, or both. Mice that are triply deficient in Nlgs 1–3 die immediately after birth due to respiratory failure, likely as a consequence of reduced synaptic transmission in the brainstem centers controlling respiration (Varoqueaux et al., 2006). Unexpectedly, however, brain cytoarchitecture and synapse density were not visibly altered, indicating that Nlgs are dispensable for the initial formation of synapses in vivo, and rather, control synaptic function. The differentiation and maturation of central synapses in the brain is technically difficult to analyze at the single-synapse level and particularly might be subject to compensatory regulations. It would thus be desirable to also explore the function of Nlgs in synaptic differentiation/maturation and its relation to Nrxs at a genetically accessible and comparatively simple synaptic terminal.

In a large-scale, unbiased mutagenesis screen for genes that regulate synaptic terminal growth in *Drosophila*, we isolated mutations in a *neuroligin* homolog (*dnlg1*) resulting in neuromuscular junctions (NMJs) with strongly reduced numbers of synaptic boutons. NMJ in vivo imaging showed that the structural defects in *dnlg1* mutants are due to a deficit in bouton addition, but not to subsequent deficits in bouton stability. DNlg1 is specifically expressed and functionally required at the postsynaptic side of NMJs, forming discrete clusters adjacent to, but not overlapping with, glutamate receptor (GluR) clusters. Lack of DNlg1 provoked severe deficits in postsynaptic differentiation, with individual active zones (AZs) or even entire boutons lacking postsynaptic GluR fields. The phenotypes identified by this analysis might be valuable for the further mechanistic analysis of Nlg-mediated signaling, and might shed light on Nlg-associated diseases such as autism (Jamain et al., 2003; Laumonnier et al., 2004).

RESULTS

Mutations in *Drosophila neuroligin 1* Identified by an Unbiased Screen for NMJ Morphology Defects

Drosophila NMJs consist of chains of synaptic boutons. Each bouton contains 30–40 individual transmitter-release sites, or synapses (Atwood et al., 1993; Jia et al., 1993). Synapses comprise a presynaptic AZ apposed by an individual postsynaptic density (PSD) (Collins and DiAntonio, 2007). During postembryonic development, synaptic terminals of NMJs gain in complexity, and the number of synaptic boutons increases dramatically in order to provide enough neurotransmitter for the growing muscle fibers (Lnenicka and Mellon, 1983). The expansion of NMJs is also subject to activity-dependent mechanisms (Griffith and Budnik, 2006; Collins and DiAntonio, 2007).

In a forward genetic screen for genes that regulate the growth of NMJs (Aberle et al., 2002) using ethyl methanesulfonate (EMS) as a chemical mutagen, we identified a complementation group of eight mutants with NMJs clearly smaller than normal (Figures 1A–1C). Using chromosomal deficiencies, meiotic recombination, and single-nucleotide polymorphisms, we mapped the mutations to the annotated gene CG31146 (Drysdale, 2008). The protein encoded by CG31146 displays strong homology to vertebrate Nlgs (Figures 1D and 1E). We therefore named this locus *Drosophila neuroligin 1* (*dnlg1*), owing to the presence of three additional *neuroligin* family genes in the *Drosophila* genome (Figure S1, available online) (Biswas et al., 2008).

The *dnlg1* locus is localized at the cytological position 84D11–84D12 of the third chromosome. The previously isolated *dnlg1* cDNA clone RE29404 encompassed 5996 bps, including an unusually long 5′ UTR (765 bps) (Stapleton et al., 2002). Sequencing of RT-PCR products derived from total embryonic RNA confirmed the annotated gene model (Figure 1D). The only difference we found was an alternative splice site in the 5′ UTR, which removes nucleotides 106–315 of exon 1 in roughly 50% of the *dnlg1* transcripts but has no effect on the coding region or the proposed translational start site in exon 2 (Figure 1D).

The cDNA encoded a transmembrane protein of 1354 aa (Figure 1E). The extracellular domain of DNlg1 contains an N-terminal signal peptide and an acetylcholinesterase-like domain (Figure 1E). Similar to known Nlgs, this domain is likely to be enzymatically nonfunctional, because the catalytic triad S-E-H of acetylcholinesterases is changed to S-E-M (S366, E495, M609) in DNlg1 (Gilbert and Auld, 2005). The cytoplasmic domain contains a PDZ-domain-binding motif at the very C terminus.

We sequenced the coding region and identified several EMS-induced point mutations in our *dnlg1* alleles (Y189H in K1809; K242Stop in I960; L319 splice site mutation in H324; L849Q in F1109; C934Stop in H703) (Figure 1E). Any transheterozygous combination between these alleles was viable.

Lack of *dnlg1* Results in a Severe Reduction of Bouton Numbers at NMJs

We quantified morphometric parameters of mutant NMJs in different alleles. The number of synaptic boutons (measured on muscle pair 1/9 and normalized to the combined muscle surface area) was reduced by approximately 50% in any mutant allele combination tested (5.3 ± 0.2 boutons per 10^4 μm^2 muscle area in wild-type versus 2.4 ± 0.1 in $dnlg1^{I960}$/Df(3R)Dsx29 mutants [n = 40, ±SEM]) (Figure 1F). The reduction in bouton number was not a secondary consequence of fewer synaptic branches, because terminal axon branching was not affected (data not shown). However, when we calculated the average number of boutons normalized to synaptic branch length (Figure 1G), bouton density on muscles 1/9 was significantly decreased in *dnlg1* mutants (1.4 ± 0.1 boutons in $dnlg1^{I960}$/Df(3R)Dsx29 per 10 μm branch length versus 2 ± 0.1 boutons in wild-type [n = 40, ±SEM]). We also measured the average diameter of the largest bouton within a given NMJ (Figure 1H). The bouton diameter on muscles 1/9 was slightly but significantly increased in *dnlg1* mutants (6.4 ± 0.1 μm in wild-type versus 7.6 ± 0.1 in $dnlg1^{I960}$/Df(3R)Dsx29 mutants [n = 40, ±SEM]).

To create an undisputable null allele, we took advantage of piggyBac elements containing FRT sites and generated three excision alleles ($dnlg1^{ex1.9}$; $dnlg1^{ex2.3}$; $dnlg1^{ex3.1}$; Figure 1D). In $dnlg1^{ex3.1}$, the entire open reading frame of *dnlg1* is eliminated. Combinations of these excision alleles in *trans* to the EMS-induced alleles $dnlg1^{I960}$ and $dnlg1^{H324}$ led to unambiguously small NMJs (Figures 1F–1H). Therefore, $dnlg1^{ex3.1}$ homozygous mutant junctions were not smaller than EMS-allele combinations (Figures 1F–1H). Thus, among the EMS alleles, $dnlg1^{I960}$ and $dnlg1^{H324}$ represent very strong hypomorphic alleles or most likely null alleles. In conclusion, elimination of *dnlg1* function leads to a severe loss of synaptic boutons at NMJs of mature *Drosophila* larvae.

NMJs of *dnlg1* Mutants Initially Form, but Lack Bouton Addition throughout Development

NMJs normally form during stages 16–17 of embryonic development. To visualize embryonic NMJs, we used an antibody against the *Drosophila* vesicular glutamate transporter (DVGLUT) (Mahr and Aberle, 2006). Size and shape of developing NMJ terminals was similar in wild-type and *dnlg1* mutant embryos (Figure S2). Thus, initial formation of synaptic terminals seems to proceed normally in the absence of DNlg1. During

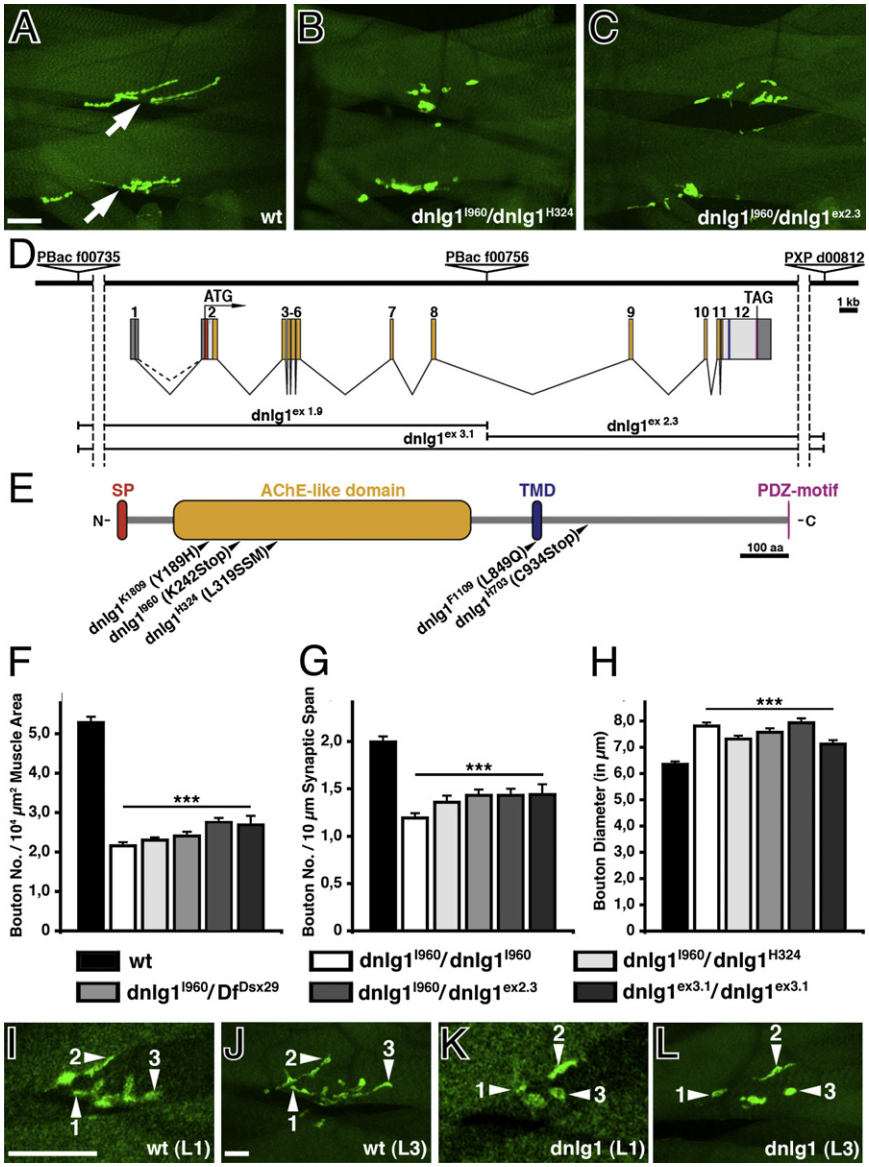

Figure 1. Mutations in *dnlg1* Cause Smaller NMJs

(A–C) Confocal micrographs of NMJs labeled with the postsynaptic marker CD8-GFP-Sh. (A) Wild-type NMJs on dorsal muscle pairs 1/9 (upper arrow) and 2/10 (lower arrow). (B) NMJs on muscles 1/9 and 2/10 are clearly smaller in $dnlg1^{l960}/dnlg1^{H324}$ mutant larvae. (C) Larvae transheterozygous for an excision allele and an EMS allele ($dnlg1^{ex2.3}/dnlg1^{l960}$) show a similar NMJ phenotype.

(D and E) Genomic locus of *dnlg1* (CG31146). (D) Exons are color coded according to the protein domains they encode. Positions of insertion elements, and dimensions of resulting excisions are indicated. Combining ex1.9 and ex3.1 specifically removes only *dnlg1*. (E) The *dnlg1* locus encodes a 1354 aa protein comprising a signal peptide (SP), an acetylcholinesterase-like domain (AChE), a transmembrane domain (TMD), and a C-terminal PDZ-domain-binding motif. The EMS-induced point mutations in the respective alleles are indicated. SSM, splice site mutation.

(F–H) Morphometric analysis of *dnlg1* mutant NMJs on muscles 1/9. (F) Quantification of the bouton number adjusted to the muscle surface area in wild-type and several *dnlg1* mutant genotypes, as indicated. (G) Quantification of bouton number per 10 µm synaptic branch length. Bouton density is decreased in *dnlg1* mutants. (H) Quantification of the average diameter of the largest bouton in a given terminal. Data shown are means ± SEM; n = 40 hemisegments; ***$p \leq 0.001$ (Mann-Whitney U-Test).

(I and J) Identified wild-type NMJs innervating muscles 1/9 imaged at the first (I) and third (J) instar stage in the same animal. Synaptic boutons are constantly added to existing synaptic branches (identified by numbered arrowheads).

(K and L) NMJs on dorsal muscles 1/9 of a $dnlg1^{l960}$ mutant larva at the first (K) and third (L) instar stage. Very few boutons are added.

Scale bars: 50 µm (A) and 20 µm (I and J). See also Figures S1 and S2.

subsequent larval stages, however, NMJs appeared smaller in *dnlg1* mutants. This phenotype per se might be due to reduced addition of synaptic boutons or, alternatively, increased retraction of established boutons. To distinguish between these possibilities, we observed NMJ development directly by imaging NMJs on dorsal muscles 1/9 in living larvae using the postsynaptic marker CD8-GFP-Sh (Zito et al., 1999) (Figures 1I–1L). Wild-type NMJs generally expand during larval development, with only a small fraction of synaptic branches (17.5%, n = 25 hemisegments) not growing (Figures 1I and 1J). In *dnlg1* mutants, the percentage of nongrowing branches was significantly increased (74.6%, n = 30 hemisegments) (Figures 1K and 1L). Even when growth did occur, it never reached the size observed at wild-type NMJs. Importantly, none of the terminals present in first-instar larvae retracted (Figures 1K and 1L). Even single and isolated boutons remained throughout the larval instars, indicating that NMJ stability was not affected. Thus, DNlg1 is required for effective addition of synaptic boutons at developing NMJ terminals.

Neurotransmission at *dnlg1* Mutant NMJs Is Reduced in Accord with Reduced Synapse Numbers

Does the loss of synaptic boutons lead to a reduction in neurotransmitter release? Usually, the number of synaptic boutons scales with the number of individual synapses present per NMJ terminal. In fact, when we quantified individual release sites apposed to GluR fields on muscle 6 using antibodies directed against the AZ protein Bruchpilot (BRP) and the GluR subunit IID (GluRIID) (Featherstone et al., 2005; Qin et al., 2005; Wagh et al., 2006), their number was strongly reduced in *dnlg1* mutants (Figure 2A) (502 ± 24 synapses in controls [n = 9] compared with 219 ± 8 in $dnlg1^{l960}/dnlg1^{H324}$ mutants [n = 9]; $p < 0.0001$).

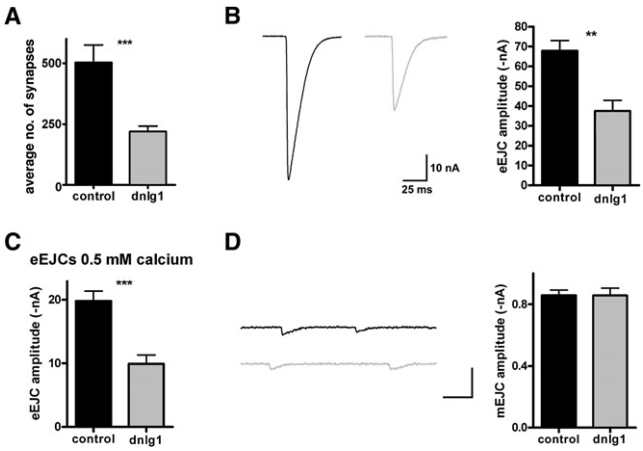

Figure 2. Fewer Synapses and Reduced Evoked Excitatory Current Amplitudes at *dnlg1* Mutant NMJs

(A) Synapse numbers are strongly reduced in *dnlg1* mutants. Synapses on muscle 6 of control (black) and $dnlg1^{I960}/dnlg1^{H324}$ mutant (gray) larvae were labeled with anti-BRP and anti-GluRIID antibodies. Synapses were counted using Imaris software.

(B–D) Electrophysiological analysis of control and *dnlg1* mutant NMJs on muscles 6/7 of third-instar larvae. (B) Left panel shows representative traces of the amplitudes of evoked excitatory junctional currents (eEJC; in nA) at 1 mM extracellular Ca^{2+} concentration. Right panel: bar graphs of mean eEJC amplitudes. (C) Bar graphs of mean eEJC amplitudes at 0.5 mM extracellular Ca^{2+} concentration. (D) Left panel shows representative traces of miniature excitatory junctional currents (mEJC). Right panel: bar graphs of mean values of mEJC amplitudes. Controls: CD8-GFP-Sh/mef2-Gal4, CD8-GFP-Sh; mutants: CD8-GFP-Sh, mef2-Gal4, $dnlg1^{H324}$ /CD8-GFP-Sh, $dnlg1^{I960}$.

Error bars = SEM, $^{**}p \leq 0.01$ (Mann-Whitney U-Test).

We wondered whether this would be reflected in reduced neurotransmission. Thus, we first examined both the spontaneous and the evoked release using intracellular recordings at 1 mM Ca^{2+} concentrations. Compared with control third-instar larvae, the evoked excitatory junctional currents (eEJC) from NMJs innervating muscles 6/7 were reduced by nearly 50% in *dnlg1* mutants (Figure 2B) (68 ± 5 nA in controls [n = 9] versus 37 ± 5 nA in $dnlg1^{I960}/dnlg1^{H324}$ mutants [n = 12]; p = 0.0016). The eEJC amplitudes were reduced to a similar extent when measured at 0.5 mM extracellular Ca^{2+} concentration (Figure 2C) (20 ± 2 nA in controls [n = 9] compared with 10 ± 1 nA in $dnlg1^{I960}/dnlg1^{H324}$ mutants [n = 11]; p = 0.0009). At the same time, the amplitude of spontaneous miniature excitatory junctional currents (mEJC) appeared unchanged at mutant NMJs (Figure 2D) (0.86 ± 0.03 nA in controls [n = 14] compared with 0.86 ± 0.05 nA in $dnlg1^{I960}/dnlg1^{H324}$ mutants [n = 16]; p = 0.9). The mEJC frequency showed a trend toward smaller values in mutant cells; however, this trend was statistically not significant (1.9 ± 0.2 Hz in controls [n = 14] compared to 1.5 ± 0.2 Hz in $dnlg1^{I960}/dnlg1^{H324}$ mutants [n = 16]; p = 0.17). Thus, our electrophysiological analysis indicates that *dnlg1* mutant NMJ terminals release less neurotransmitter per action potential. This reduction seems proportional to the reduction of synapses present at these terminals (compare Figures 2A and 2B). Because we also did not observe any changes in functional parameters such as Ca^{2+} dependence of release, the structural reduction in the number of release sites seems to be responsible for the reduction in transmitter release, while the synapses remaining at *dnlg1* mutant NMJs appear largely functional.

Defects of Postsynaptic Differentiation at *dnlg1* Mutant Boutons

To investigate possible presynaptic or postsynaptic differentiation defects, we performed light microscopic analysis of *dnlg1* mutant terminals. First, the presynaptic vesicle protein Synaptotagmin (Syt) and cytoskeleton marker Ankyrin 2 (Ank2) (Koch et al., 2008) were stained together with CD8-GFP-Sh, which marks the subsynaptic reticulum (SSR) (Figures 3A–3D). The SSR consists of membranous invaginations of the muscle plasma membrane and surrounds the postsynaptic GluR fields. Notably, we found many areas where apparently mature presynaptic boutons, as highlighted by the accumulation of Syt and Ank2, were not apposed by CD8-GFP-Sh signals (compare arrows in Figure 3D). Quantified, 46% of NMJs on muscles 1/9 possessed obvious postsynaptic differentiation defects, compared with only 5% in control larvae (n = 20). These mismatches did not include the entire branch because a majority of boutons still maintained close apposition of the presynaptic and postsynaptic membranes. Rather, mismatches affected a subset of boutons, regardless of whether they were localized in proximal or distal branch regions. These results indicate that a fraction of fully differentiated presynaptic boutons face a postsynaptic site that lacks SSR.

To discriminate assembly deficits from secondary stabilization defects, we performed in vivo live imaging of *dnlg1* mutant terminals expressing a BRP fragment highlighting presynaptic AZs (Schmid et al., 2008) together with the postsynaptic marker CD8-GFP-Sh (Figures 3E and 3F). Growing boutons normally contain AZs, T-bars, and synaptic vesicles, and are surrounded by SSR membranes (Zito et al., 1999) (Figure 3E). In contrast, a subset of presynaptic boutons in *dnlg1* mutants continuously added AZ material but failed to differentiate an apposing postsynaptic domain, as indicated by the complete lack of the CD8-GFP-Sh signal (arrows in Figure 3F). The number of unapposed BRP spots increased over time (t = 0 hr: 7.39 ± 0.71; t = 12 hr: 9.06 ± 1.34; t = 24 hr: 10.88 ± 1.23 BRP spots per bouton lacking SSR membranes [n = 9 boutons on muscles 1/9]). Overall, the lack of postsynaptic SSR reflects a genuine inability to assemble postsynaptic structures at *dnlg1* boutons.

GluR Accumulation Defects in the Absence of DNlg1

Next, we asked whether apart from the SSR defects the accumulation of postsynaptic proteins—particularly of postsynaptic GluRs—would be affected. We subjected control (Figures 4A and 4C) and *dnlg1* mutant terminals (Figures 4B and 4D–4G) to an extensive immunohistochemical analysis. Normally, the AZ marker BRP localizes opposite GluR clusters at mature NMJs (Figures 4A and 4C). At *dnlg1* mutant NMJs, however, we could readily identify presynaptic areas that lacked postsynaptic domains, as indicated by BRP-positive punctae not apposed by GluRs (arrows in Figures 4B, 4D, and 4E). Frequently, individual AZs or groups of AZs lacking GluRs were present (arrows in Figures 4D and 4E). "Orphan" boutons, i.e., differentiated

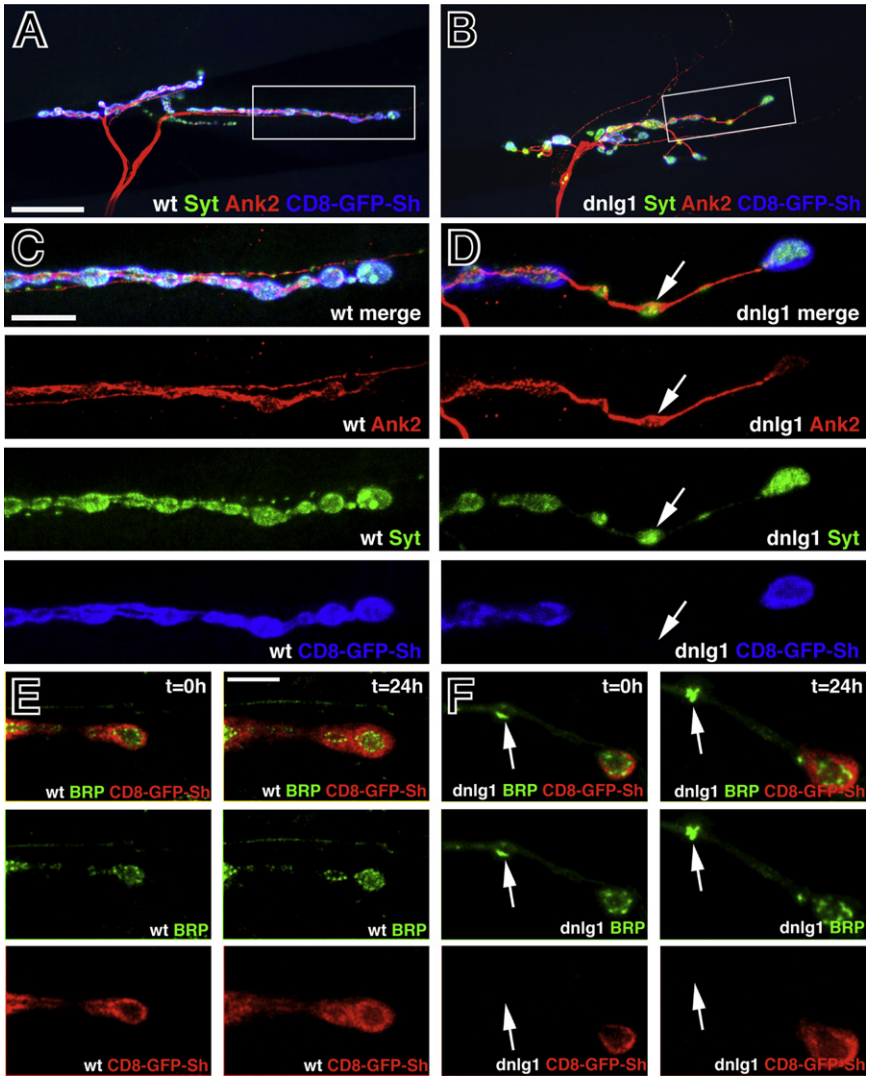

Figure 3. Fully Differentiated Presynaptic Boutons Are Not Apposed by Postsynaptic Specializations in *dnlg1* Mutants

(A–D) Wild-type NMJs on muscles 1/9 (A and C) compared with *dnlg1*^{I960}/Df(3R)Dsx29 mutant NMJs (B and D). The overviews (A and B) highlight the presynaptic markers Synaptotagmin (Syt, green) and Ankyrin 2 (Ank2, red), and the postsynaptic marker CD8-GFP-Sh (blue). Boxed regions are enlarged. (C) Synaptotagmin labels synaptic vesicles accumulating in presynaptic boutons. Ankyrin 2 forms a cytoskeletal lattice that is typically unfolded in major boutons. CD8-GFP-Sh reveals the outline of the postsynaptic subsynaptic reticulum. Merged images show that postsynaptic regions are normally strictly apposed to presynaptic boutons at wild-type NMJs. (D) Fully differentiated presynaptic regions of *dnlg1* mutant NMJs not apposed by postsynaptic domains (compare arrows in D).

(E and F) In vivo image of identified NMJs in wild-type and *dnlg1*^{I960}/*dnlg1*$^{ex2.3}$ mutant third-instar larvae at two different time points. AZs are labeled with a fluorescently tagged fragment of BRP (BRP-short-Strawberry, green) and SSR membranes, with CD8-GFP-Sh (red). (E) At control NMJs, all BRP-positive puncta develop in the postsynaptic zone within a 24 hr time interval. (F) Imaging of *dnlg1* mutant NMJs within a 24 hr time interval reveals continuous clustering of presynaptic AZ material in boutons lacking postsynaptic markers (arrows in F).

Scale bars: 30 μm (A), 10 μm (C), and 5 μm (E).

presynaptic boutons entirely lacking postsynaptic GluRs, occurred with a frequency of about 8% of *dnlg1* mutant boutons, but were not found in control NMJs (Figure 4H). The severity and frequency of these phenotypes were independent of the *dnlg1* alleles used and were also observed in *dnlg1*^{H703}, which contains a stop codon in the cytoplasmic domain, suggesting that this domain plays an important role in the assembly of PSDs (Figure S3). Other postsynaptic markers, namely the PSD marker Pak and the SSR marker Spectrin, were absent in orphan boutons as well (Figure S4). Thus, DNlg1 seems to promote the accumulation of postsynaptic GluRs as well as SSR differentiation at neuromuscular terminals.

Electron Micrographs Reveal Synaptic Membrane Detachments and Postsynaptic Differentiation Defects

At the fly NMJ, synapses are characterized by planar, 100–500 nm wide appositions of presynaptic and postsynaptic membranes (Figure 5A, arrowheads) decorated by T-bars. Lateral to synapses, bouton membranes are not entirely aligned in parallel, but rather form punctate contacts. In electron micrographs, we found that presynaptic AZs still formed in *dnlg1* mutant boutons (arrowheads in Figure 5B). Mutant AZs contained T-bars and clustered synaptic vesicles. Synaptic vesicles were present at roughly normal size and density, with large vesicle diameters in slightly higher numbers than normal (35.31 ± 0.25 nm in controls [n = 410 vesicles] versus 36.88 ± 0.55 nm in *dnlg1*^{I960}/*dnlg1*^{H324} mutants [n = 362 vesicles]; p = 0.0049, Student's t test).

Notably, we observed a subset of mutant boutons with a reduction in the thickness of the SSR. In fact, the relative SSR area was significantly reduced in *dnlg1* NMJs (wild-type 2.22 ± 0.34, n = 19; *dnlg1*^{I960}/*dnlg1*^{H324} 1.27 ± 0.16, n = 26; p = 0.0083, Student's t test) (Figure 5G). In extreme cases, boutons appeared to be in "direct contact" with the contractile filaments (arrowheads in Figure 5C). Importantly, however, even at places without SSR, AZs were still present and maintained the tight apposition of presynaptic and postsynaptic membranes, indicating that synapse formation per se appeared not to be affected (Figure 5C). Thus, molecular and ultrastructural data agree that the differentiation of postsynaptic domains is affected in *dnlg1* mutants. Surprisingly, even at places where postsynaptic SSR differentiation largely failed, basic aspects of synapse formation seemed to proceed.

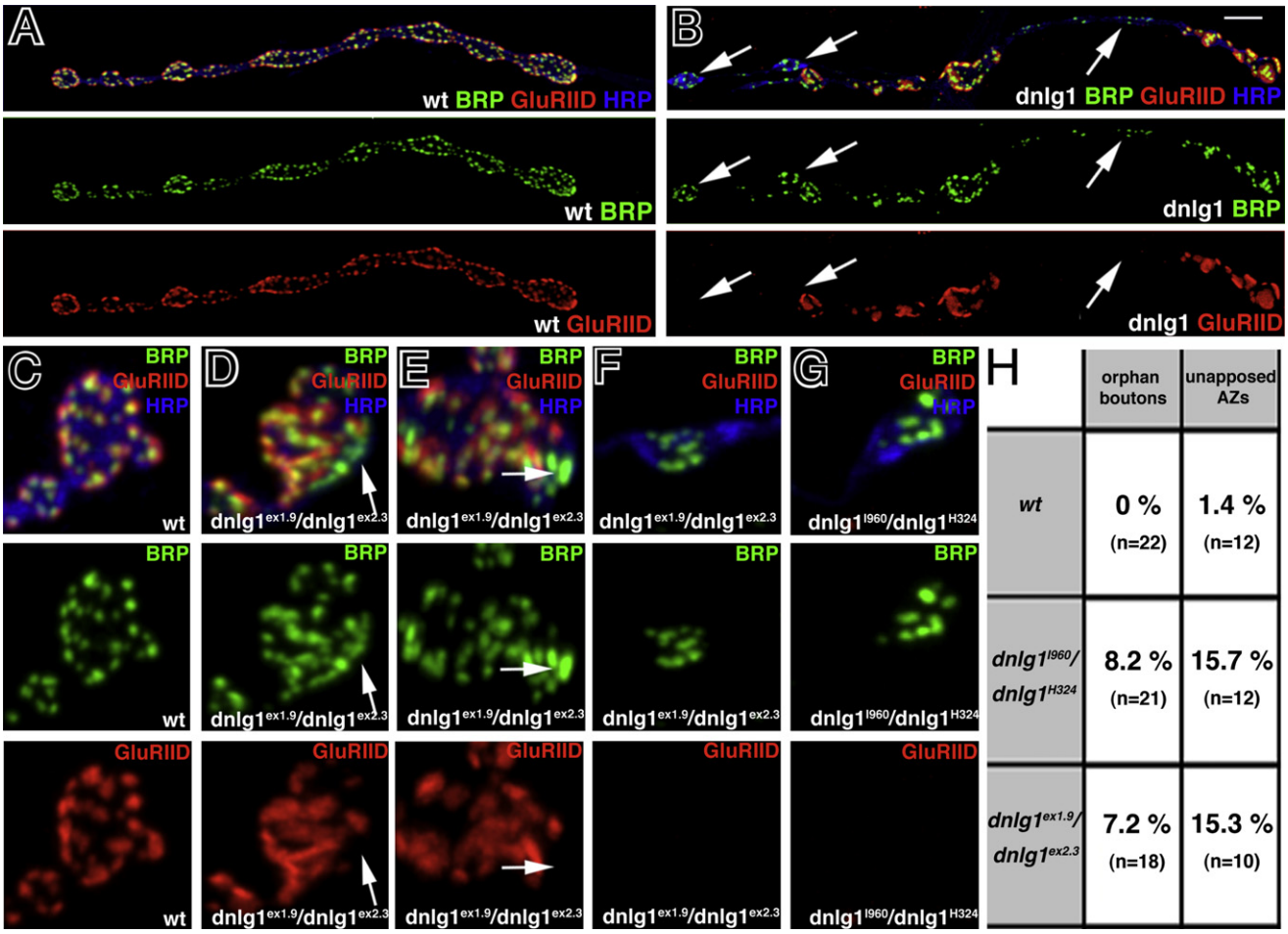

Figure 4. Misalignment of Presynaptic Transmitter Release Sites and Postsynaptic GluR Fields in *dnlg1* Mutants

(A and B) Wild-type (A) and *dnlg1*$^{ex1.9}$/*dnlg1*$^{ex2.3}$ mutant (B) NMJs stained with antibodies recognizing neuronal plasma membrane (HRP), AZ marker Bruchpilot (BRP), and GluR subunit GluRIID. The merged image in (B) shows presynaptic AZs not apposed to postsynaptic receptor fields (arrows).

(C–G) Wild-type (C) and *dnlg1* mutant boutons (D–G) triple labeled with antibodies recognizing BRP, GluRIID, and HRP. In *dnlg1*$^{ex1.9}$/*dnlg1*$^{ex2.3}$ mutant boutons, a subset of AZs are not apposed by corresponding GluRs (arrows in D and E). Orphan boutons, presynaptic boutons entirely lacking postsynaptic GluRs, occur only in *dnlg1* mutants, irrespective of the alleles used (*dnlg1*$^{ex1.9}$/*dnlg1*$^{ex2.3}$ in F, *dnlg1*^{l960}/*dnlg1*^{H324} in G).

(H) Quantification of orphan boutons and AZs unapposed by receptor fields in controls and two allelic *dnlg1* combinations. Whereas orphan boutons are not found in controls, approximately 8.2% of presynaptic boutons on muscle 4 completely lack apposed GluRs in *dnlg1*^{l960}/*dnlg1*^{H324} mutants. Unapposed AZs occurred with a frequency of 15.7%.

Scale bar: 5 μm (B). See also Figures S3 and S4.

Postsynaptic DNlg1 Clusters Localize Adjacent to GluR Fields

Where is DNlg1 expressed to regulate bouton addition and postsynaptic differentiation? To answer this question, we first performed in situ hybridization experiments. Antisense probes synthesized from clone RE29404 recognized endogenous *dnlg1* transcripts in somatic muscles (Figures 6A and 6B), whereas sense probes did not. We first detected expression at late stage 12 in a subset of myoblasts, the progenitor cells of body wall muscles. At stage 14, most myoblasts expressed *dnlg1* (Figure 6A). At the end of embryogenesis, *dnlg1* was also expressed in the dorsal pharyngeal muscles and the ring gland. We were unable to detect any expression in the central nervous system (arrowhead in Figure 6B).

To investigate the subcellular distribution of DNlg1, we raised a polyclonal antiserum against a C-terminal peptide (see Experimental Procedures). The affinity-purified antiserum clearly highlighted NMJs in wild-type larvae (Figures 6C and 6D). In contrast, NMJs in *dnlg1* mutants were not stained and only background signals remained, demonstrating the specificity of the antibody (Figures 6E and 6F). For unequivocally demonstrating postsynaptic expression, endogenous DNlg1 was downregulated specifically either on the presynaptic or postsynaptic side using transgene-mediated RNAi in combination with the UAS/Gal4 system (Brand and Perrimon, 1993; Dietzl et al., 2007). While presynaptic expression using elav-Gal4 did not interfere with the antibody signal at NMJs (Figures 6G and 6H), expression in postsynaptic muscles using mef2-Gal4 completely

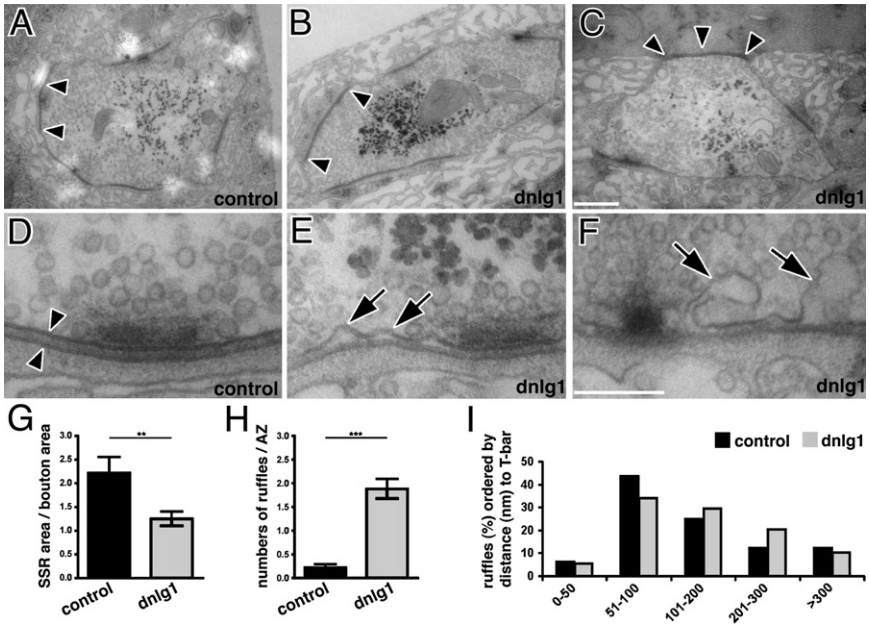

Figure 5. Electron Micrographs Reveal Postsynaptic Differentiation Defects and Synaptic Membrane Detachments in *dnlg1* Mutant Boutons

(A–C) Electron micrographs of control (A) and *dnlg1*^{I960}/*dnlg1*^{H324} (B and C) boutons on muscle 6. AZs with T-bars are marked (arrowheads). (C) AZ (arrowheads) not surrounded by SSR but facing contractile muscle filaments.

(D–F) AZs in wild-type (D) and *dnlg1*^{I960}/*dnlg1*^{H324} mutant (E and F) boutons. AZs are characterized by parallel alignment and close apposition of presynaptic and postsynaptic membranes (arrowheads). (E and F) Presynaptic plasma membranes frequently detach from the dense material in the synaptic cleft, forming membrane ruffles (arrows).

(G–I) Quantification of ultrastructural parameters in control (w^{1118}, black) and *dnlg1*^{I960}/*dnlg1*^{H324} (gray) NMJs. (G) The relative SSR area is reduced in *dnlg1* mutants. (H) The number of membrane ruffles in AZs is strongly increased in *dnlg1* mutants. (I) The distance of these ruffles to the center of the T-bar is unchanged. Error bars = SEM, $^{**}p \leq 0.01$ (Student's t test).

Scale bars: 500 nm (C) and 200 nm (F).

abolished the DNlg1 clusters, confirming that they are of postsynaptic origin (Figures 6I and 6J).

Does the position of the postsynaptic DNlg1 spots relate to postsynaptic marker proteins? We stained NMJs with anti-DNlg1 and anti-GluRIID antibodies and found that DNlg1 was expressed in a spotted pattern adjacent to GluR fields (Figures 6K and 6L). Quantification showed that 69% ± 9% of all PSDs were associated with discrete DNlg1 spots (n = 1425 PSDs). We detected a similar distribution of the DNlg1 spots relative to presynaptic AZs (visualized with anti-BRP antibodies) (Figures 6M and 6N), consistent with a very high degree of AZ to PSD coordination in this system (Schmid et al., 2008). Thus, DNlg1 is specifically expressed in postsynaptic muscle cells and accumulates at NMJs, in a location adjacent to PSDs.

Postsynaptic DNlg1 Is Needed for Effective Addition of Synaptic Boutons at Developing NMJ Terminals

The specific clustering of DNlg1 adjacent to, but not within, PSDs might define a separate postsynaptic compartment at *Drosophila* NMJs. To test whether DNlg1 is functionally required at these postsynaptic sites, we attempted to eliminate *dnlg1* expression in selected tissues using RNAi. As mentioned above, all allelic combinations (early stop codons or full deletions) invariably resulted in unusually small NMJs, showing a 50% reduction in overall bouton numbers. To define the relevant cell compartment for DNlg1 function, we first triggered RNAi in neurons or muscles of wild-type larvae. Presynaptic knockdown of DNlg1 (using elav-Gal4) altered neither the size of NMJs (Figure S5) nor the staining of DNlg1 at NMJs (Figures 6G and 6H). In contrast, when DNlg1 function was eliminated in muscles (using mef2-Gal4), NMJ size was drastically reduced (Figure S5). This is in line with the elimination of DNlg1 staining at NMJs upon knockdown of DNlg1 in muscles (Figures 6I and 6J).

We also tested for tissue-specific functions in genetic rescue experiments (Figure 7). For this purpose, we expressed a wild-type *dnlg1* cDNA in muscles or neurons in *dnlg1* mutant backgrounds. To increase detection sensitivity, we labeled DNlg1 with GFP in a juxta-membrane position, because this location is predicted not to interfere with protein function (Dresbach et al., 2004; Wittenmayer et al., 2009) (Figure 7A). Full-length DNlg1-GFP, when expressed with mef2-Gal4 in a mutant background, rescued the small terminal phenotype back to control levels (Figures 7E and 7K). In contrast, expression of DNlg1-GFP in all postmitotic neurons using elav-Gal4 did not substantially improve the synaptic phenotype of *dnlg1* mutants (Figures 7D and 7K). Thus, DNlg1 is not only expressed in muscle fibers, but its functional expression within fibers is also required for effective formation of synaptic boutons at developing and maturing NMJs.

Lack of the Cytoplasmic Domain of DNlg1 Provokes Strong Dominant-Negative Effects

We next created transgenic lines expressing deletion constructs of DNlg1 based on DNlg1-GFP to isolate the domains important for DNlg1 function (Figure 7A). First, a construct lacking the extracellular domain but retaining the transmembrane and cytoplasmic domains (DNlg1-GFP$^{\Delta extra}$) was overexpressed under control of mef2-Gal4 specifically in muscles. While DNlg1-GFP$^{\Delta extra}$ localized to NMJs, it had no effect on NMJ morphology (Figures 7I and 7L). In addition, DNlg1-GFP$^{\Delta extra}$ expression in muscles of *dnlg1* mutants did not substantially rescue the null mutant phenotypes (Figures 7F and 7K). Notably, however, DNlg1-GFP$^{\Delta cyto}$ (Figure 7A) lacking the cytoplasmic domain provoked very small NMJs when expressed in wild-type muscles (Figures 7J and 7L). In fact, NMJs were even slightly smaller than those in the null phenotypes (Figure 7C). When expressed in a *dnlg1* mutant background, DNlg1-GFP$^{\Delta cyto}$ not only failed to rescue the number of synaptic boutons and the size of NMJs,

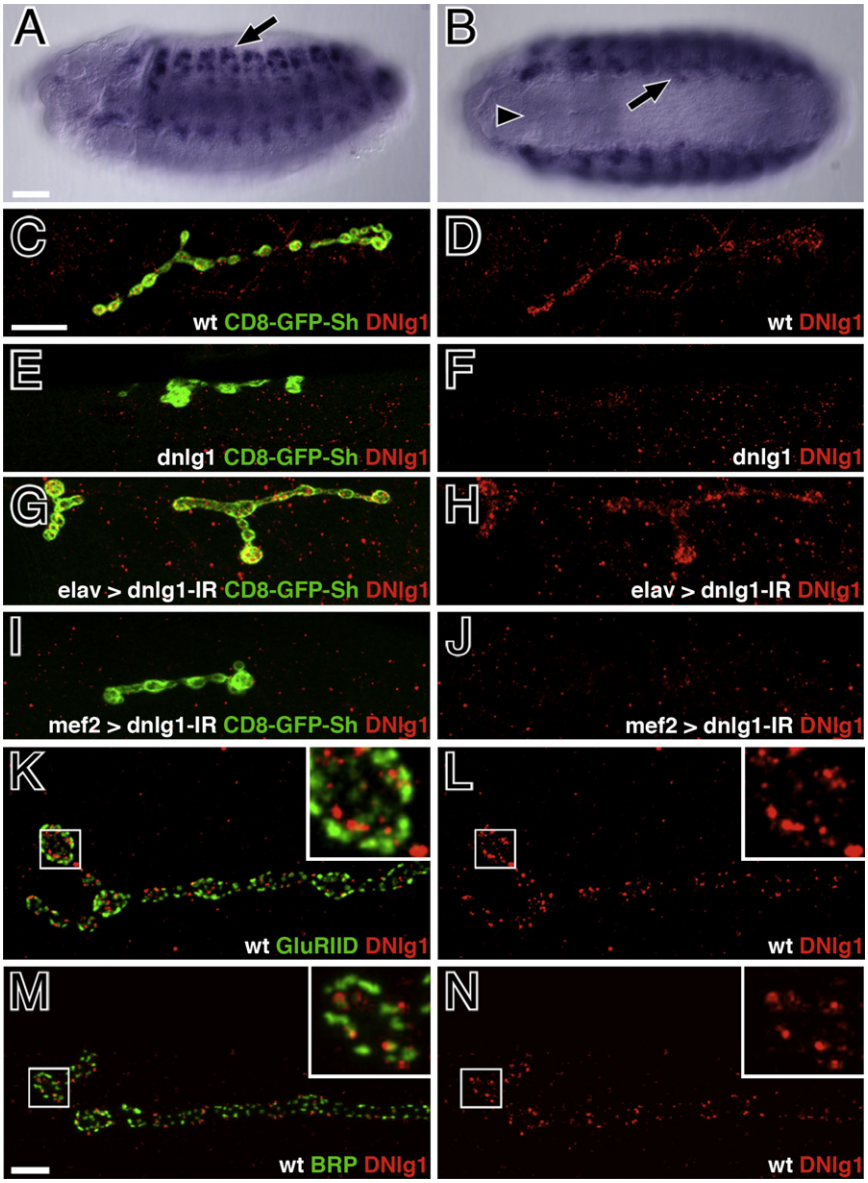

Figure 6. DNlg1 Localizes in Discrete Spots Adjacent to Postsynaptic GluRs

(A and B) In situ hybridizations labeling *dnlg1* mRNA in wild-type embryos at stage 14. (A) Lateral view showing *dnlg1* expression in differentiating myoblasts (arrow). (B) Ventral view showing expression in developing muscle fibers (arrow) but not in the ventral nerve cord (arrowhead: ventral midline).

(C–J) Confocal micrographs of NMJs (muscle 4) labeled by CD8-GFP-Sh and anti-DNlg1 staining. (C and D) DNlg1 antiserum recognizes a punctate pattern at wild-type, but not at *dnlg1*^{1960}/Df(3R)Dsx29 mutant, NMJs (E and F). (G and H) Control NMJs expressing UAS-*dnlg1*-IR in all postmitotic neurons using elav-Gal4. DNlg1 is still expressed and NMJs appear normal. (I and J) NMJs of a wild-type larva expressing UAS-*dnlg1*-IR specifically in muscles using mef2-Gal4. The postsynaptic RNAi effect abolishes the expression of DNlg1 and provokes smaller NMJs. (K and L) Wild-type NMJs stained with anti-DNlg1 and anti-GluRIID antibodies. DNlg1 shows a punctate pattern (L) that is adjacent to postsynaptic GluRs (inset in K).

(M and N) Control NMJs stained with anti-DNlg1 and anti-BRP antibodies. Postsynaptic DNlg1 punctae (N) localize adjacent to presynaptic BRP punctae (inset in M).

Scale bars: 50 μm (A), 20 μm (C), and 5 μm (M). See also Figure S5.

but also produced NMJs even smaller than those in null mutants (compare Figure 7C and 7G). Likely, DNlg1-GFP$^{\Delta cyto}$ can still attach to signaling partners via its extracellular region, transmembrane region, or both (because it effectively localizes to NMJs). Due to the lack of its cytoplasmic domain, we suppose it renders these complexes nonfunctional, in effect acting as a dominant-negative protein. Since only DNlg1-GFP was able to rescue the mutant phenotype, we conclude that both the extracellular and the cytoplasmic domain appear to be essential for DNlg1 signaling.

Ectopic Postsynaptic Differentiation Triggered by Increased Amounts of DNlg1

While DNlg1-GFP was expressed, we found further evidence that DNlg1 is important for postsynaptic assembly. Apart from type I NMJ innervations, larval muscles also receive innervation by thin-diameter type II terminals (Hoang and Chiba, 2001). While normally these lack SSR, and hence typical postsynaptic markers of type I boutons such as CD8-GFP-Sh or Discs large (Dlg), they can be labeled with anti-HRP antibodies (Jia et al., 1993). Notably, after muscle expression of DNlg1-GFP, we noticed not only an increase of DNlg1 intensity at NMJs but also that type II terminals normally negative for the SSR marker Dlg now show Dlg expression (Figure 7N). Similarly, we could detect low levels of the GluR subunit GluRIIC, normally confined to type I boutons, at type II terminals (data not shown). This effect was specific to DNlg1, as it was not observed after expression of the synaptic adhesion protein Fasciclin II (Grenningloh et al., 1991) (Figure 7M). While DNlg1-GFP$^{\Delta cyto}$ localized to type II terminals, obviously due to the lack of its cytoplasmic domain, it failed to recruit Dlg (Figure 7O). In contrast, DNlg1-GFP$^{\Delta extra}$ did not localize to type II terminals, and consequently type II boutons lacked Dlg (Figure 7P). However, DNlg1-GFP$^{\Delta extra}$ accumulated in cytoplasmic granulae in muscle fibers that contained Dlg (Figure 7P) and GluRs (data not shown), suggesting that the cytoplasmic domain is tightly associated with these markers. Thus, DNlg1, when overexpressed, is able to ectopically recruit postsynaptic marker proteins to a terminal normally not

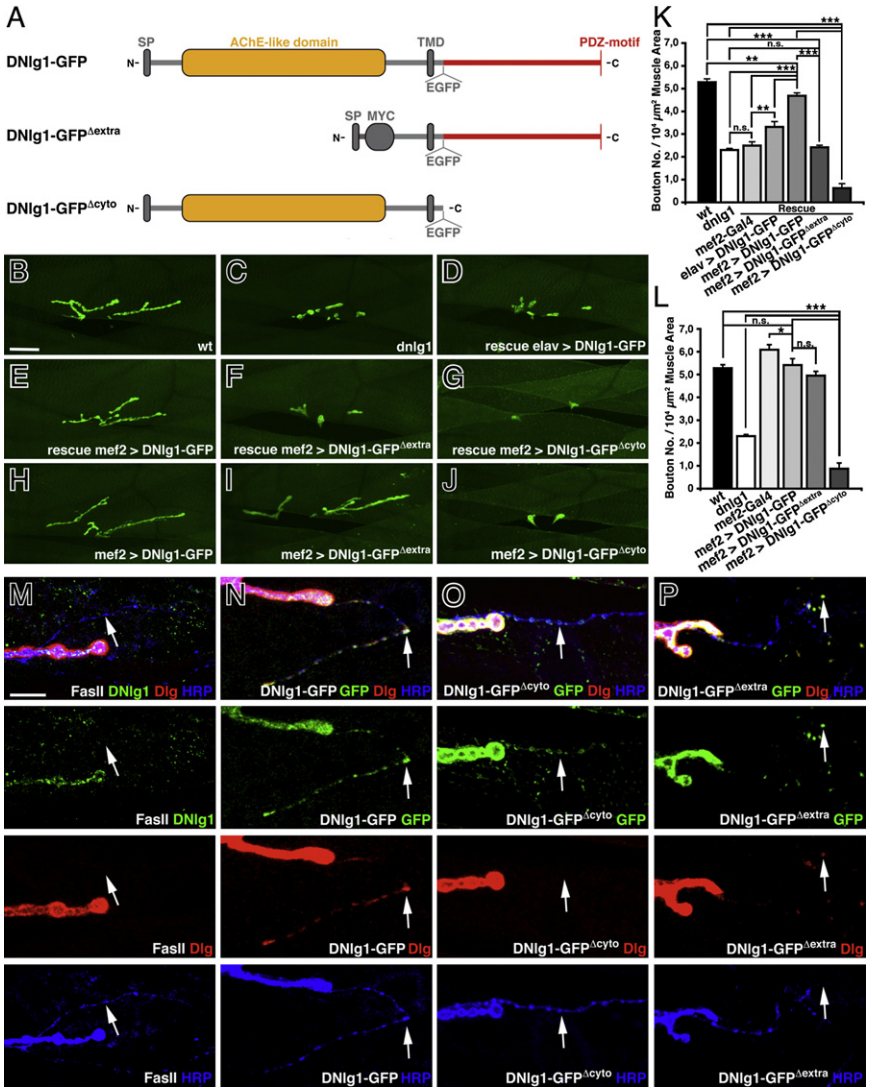

Figure 7. DNlg1 Is Functionally Required in Muscles and Induces the Differentiation of Postsynaptic Domains

(A) Schematic representation of N- and C-terminal deletion constructs of DNlg1-GFP.

(B–G) Genetic rescue experiments. Compared to *dnlg1*^{I960}/*dnlg1*^{H324} mutants (C), expression of DNlg1-GFP under control of elav-Gal4 failed to rescue the NMJ phenotypes (D). Postsynaptic expression, however, using mef2-Gal4, rescued NMJ size (E). Both DNlg1-GFP$^{\Delta extra}$ and DNlg1-GFP$^{\Delta cyto}$ failed to rescue *dnlg1* mutant NMJs when expressed in muscles (F and G). All rescue experiments were performed in *dnlg1*^{I960}/*dnlg1*^{H324} mutants expressing the CD8-GFP-Sh transgene.

(H–J) Overexpression of DNlg1-GFP (H) and DNlg1-GFP$^{\Delta extra}$ (I) in muscles of wild-type larvae using a recombinant mef2-Gal4, CD8-GFP-Sh line had no effect on NMJ size. (J) Expression of DNlg1-GFP$^{\Delta cyto}$ under control of mef2-Gal4 strongly inhibited synaptic growth.

(K and L) Quantification of bouton numbers at NMJs on muscles 1/9 in rescue (K) and overexpression (L) experiments of the indicated genotypes. Bouton numbers in control and *dnlg1*^{I960}/*dnlg1*^{H324} mutant larvae are shown for comparison. Error bar = SEM; n.s.: not significant; **p $\leq$ 0.01 (Mann-Whitney U-Test).

(M–P) The cytoplasmic domain of DNlg1 recruits Dlg, a marker for the postsynaptic SSR that normally surrounds type I, but not type II, boutons. Fasciclin II (FasII) (M), DNlg1-GFP (N), DNlg1-GFP$^{\Delta cyto}$ (O), and DNlg1-GFP$^{\Delta extra}$ (P) were expressed in muscles using mef2-Gal4. NMJs were stained with anti-HRP, anti-Dlg, and either anti-DNlg1 (M) or anti-GFP (N–P) antibodies. Type II boutons are visualized by HRP. (M) The synaptic adhesion protein FasII is unable to recruit Dlg into type II boutons (arrows). (N) DNlg1-GFP accumulates at type I and type II boutons and ectopically recruits Dlg into type II boutons (arrows). (O) DNlg1-GFP$^{\Delta cyto}$ is also expressed at type II boutons but fails to recruit Dlg (arrows). (P) DNlg1-GFP$^{\Delta extra}$ enriches at type I, but not type II, boutons, and is found in cytoplasmic granulae also positive for ectopic Dlg (arrows).

Scale bars: 50 µm (B) and 10 µm (M).

undergoing such a differentiation, again pointing toward a rate-limiting role of this protein for postsynaptic differentiation.

Presynaptic DNrx Is Essential for Effective Clustering of Postsynaptic DNlg1

Binding of Nrx via an ectodomain-ectodomain interaction is suggested to be important for Nlg function. Thus, we wanted to compare the *dnrx* and *dnlg1* mutant phenotypes directly and introduced the CD8-GFP-Sh marker into the *dnrx* mutant background (Figures 8A–8C) (Li et al., 2007; Zeng et al., 2007). Most NMJs in *dnrx* mutants were visibly smaller (Figure 8B), confirming previous observations (Li et al., 2007). Compared with various amorphic *dnlg1* alleles, however, NMJ size was less affected in *dnrx* mutants (Figure 8C). Quantitatively, bouton numbers on muscles 1/9 were reduced by 53% in *dnlg1* but only by 36% at *dnrx* mutant terminals (27.3 ± 1.1 boutons in wild-type, 12.7 ± 0.6 boutons in *dnlg1*^{I960}/Df(3R)Dsx29, and 17.5 ± 0.8 boutons in *dnrx*^{241}/Df(3R)Exel6191 [n = 40, ±SEM]) (Figures 8E and S6). To test for a possible genetic interaction, we also produced *dnrx*, *dnlg1* double mutants. These double mutants were adult viable as was each single mutant. NMJs in *dnrx, dnlg1* double mutants were indistinguishable from those of *dnlg1* single mutants (Figure 8D). Thus, further loss of *dnrx* does not add onto the bouton formation defects present in *dnlg1* mutants (Figures 8E and S6).

In another series of experiments, we overexpressed untagged, full-length DNlg1 at levels significantly higher than DNlg1-GFP

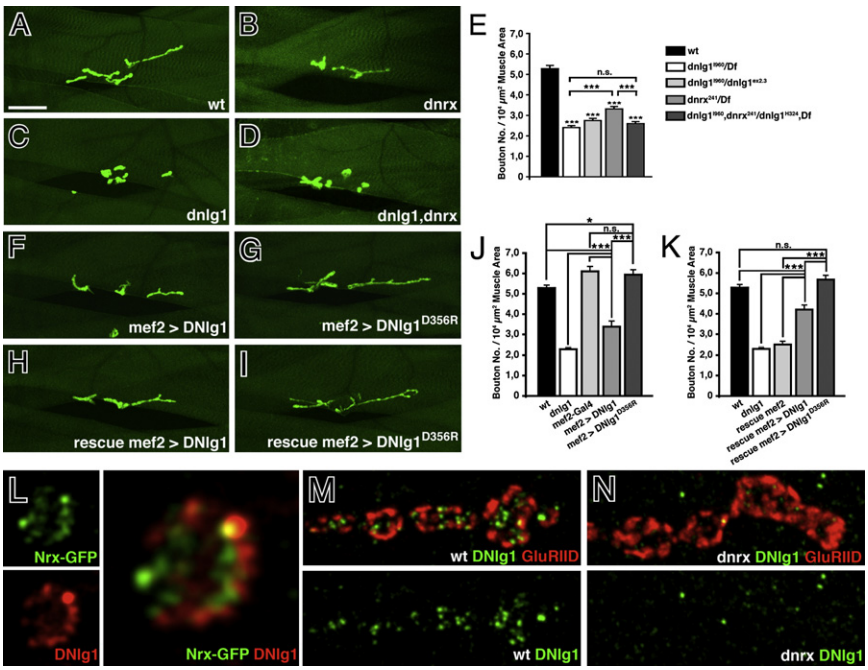

Figure 8. Role of DNrx for DNlg1 Signaling

(A–D) Comparison of NMJs on muscles 1/9 in wild-type CD8-GFP-Sh (A), *dnrx*^{241}/Df(3R)Exel6191 (B), *dnlg1*^{I960}/*dnlg1*^{H324} (C), and *dnlg1*^{I960}, *dnrx*^{241}/*dnlg1*^{H324}, Df(3R)Exel6191 (D) mutant larvae. Compared with wild-type controls, NMJ size is reduced in *dnlg1* and *dnrx* mutant larvae, while bouton spacing is affected only in *dnlg1* mutants. NMJ size is not further decreased in *dnlg1*, *dnrx* double mutants. (E) Quantification of bouton numbers (muscles 1/9) in the indicated genotypes. Error bars = SEM, n.s.: not significant, ***p ≤ 0.001 (Mann-Whitney U-Test). These values also apply to (J) and (K). (F and G) Overexpression of full-length DNlg1 at high levels using mef2-Gal4 induces a dominant-negative NMJ phenotype, with bouton numbers clearly reduced (F). Overexpression of a DNlg1 construct carrying a point mutation predicted to abolish DNrx binding does not reduce the size of NMJs (G). Both constructs were expressed from within the same genomic insertion site. For quantification see (J). (H and I) Genetic rescue experiments using mef2-Gal4 to express full-length DNlg1 at high levels improves, but does not fully rescue, the *dnlg1* mutant phenotype (H). The mutant NMJ phenotype, however, is fully rescued by the construct carrying the D356R point mutation (I). For quantification see (K). (L) Presynaptic DNrx-GFP, expressed in motoneurons of *dnrx*^{241}/Df(3R)Exel6191 mutants using OK6-Gal4, localizes in apposition to postsynaptic DNlg1 clusters. NMJs were stained with anti-GFP and anti-DNlg1 antibodies. (M and N) Endogenous DNlg1 fails to cluster adjacent to postsynaptic GluR fields in the absence of DNrx. NMJs in wild-type (M) and *dnrx*^{241}/Df(3R)Exel6191 mutants (N) stained with anti-GluRIID and anti-DNlg1 antibodies are shown. Postsynaptic DNlg1 clusters are no longer observed. Scale bar: 50 μm (A). See also Figures S6–S8.

(Figure S7). This reduced NMJ size in wild-type larvae, probably by interfering with endogenous DNlg1 complexes (Figure 8F). This dominant-negative effect was, however, not observed when we overexpressed DNlg1 in the *dnrx* mutant background (Figure S7). To further test for a possible involvement of DNrx in DNlg1 function, we introduced a point mutation into DNlg1, DNlg1^{D356R}, which by inference from mammalian data should abolish the binding to DNrx (Reissner et al., 2008). In contrast to the unmodified version, DNlg1^{D356R} overexpression in wild-type muscles did not visibly alter the structure of NMJs (both DNlg1 and DNlg1^{D356R} were expressed from the same chromosomal integration site to ensure equal expression levels) (Figure 8G). When expressed in a *dnlg1* mutant background, DNlg1^{D356R} significantly rescued the NMJ phenotype (Figure 8I). Thus, these data imply that DNrx binding via its ectodomain is not an absolute prerequisite for DNlg1 function, but rather promotes DNlg1 function.

To further compare *dnrx* and *dnlg1* mutants, we wondered whether *dnrx* mutants also display presynaptic and postsynaptic apposition defects. We therefore stained *dnrx* mutant NMJs with anti-BRP and anti-GluRIID antibodies. In contrast to *dnlg1* mutant NMJs (Figure 4), entire boutons or individual AZs lacking GluRs were not observed in *dnrx* mutants, confirming previous observations (data not shown, Li et al., 2007). Upon closer analysis, however, we recognized that postsynaptic receptor fields appeared irregular and often enlarged in both *dnlg1* and *dnrx* mutants (Figure S8). In fact, quantification after 3D reconstruction (see Supplemental Experimental Procedures) showed that the integrated GluR intensities per PSD were significantly increased in both *dnlg1* and *dnrx* mutants (Figure S8). Again, this effect was qualitatively similar but quantitatively milder in *dnrx* as compared with *dnlg1* mutants.

Further similarities were also revealed by our ultrastructural analysis of *dnlg1* mutant boutons. In control animals, AZ membranes were aligned in parallel and showed hardly any ruffles in the synaptic membranes (Figure 5D). In contrast, in *dnlg1* mutants, we found an atypical number of shallow ruffles (arrows in Figure 5E) in AZs (1.88 ± 0.21 ruffles per AZ in *dnlg1*^{I960}/*dnlg1*^{H324} compared with only 0.22 ± 0.07 in wild-type larvae [$p < 0.005$, Student's t test]) (Figure 5H). The average distance of the ruffles to the center of the T-bar was not significantly altered (wild-type 144.43 ± 23.92 nm, $n_{ruffles} = 15$, $n_{AZ} = 73$; *dnlg1*^{I960}/*dnlg1*^{H324} 158.97 ± 10.12, $n_{ruffles} = 87$, $n_{AZ} = 52$; $p = 0.57$; Student's t test) (Figure 5I). Notably, *dnrx* mutant AZs were shown previously to display similar ruffles in AZs (Li et al., 2007; Zeng et al., 2007). However, for *dnlg1* NMJs, similar but even more pronounced invaginations were readily observed (arrows in Figure 5F). Thus, mutations in *dnlg1* result in certain deficits of presynaptic assembly, obviously in a transsynaptic manner, with defects again being similar to, but apparently stronger than, those found in *dnrx*.

Due to these phenotypic similarities, DNlg1 might work in a related context, where DNrx promotes, but is not absolutely required for, DNlg1 signaling. Similar to DNlg1 (Figures 6M and 6N), DNrx was reported to cluster in discrete patches close to, but not overlapping with, presynaptic AZs (Li et al., 2007). To

perform colabeling experiments, we created a GFP-tagged version of DNrx and expressed this in presynaptic motoneurons of *dnrx* mutants. Endogenous DNlg1 and DNrx-GFP frequently were found in apposing spots on both sites of the synapse (Figure 8L). Thus, we asked whether presynaptic DNrx might be needed for effective clustering of postsynaptic DNlg1. In fact, clusters of DNlg1 adjacent to AZs were drastically reduced at *dnrx* mutant NMJs (Figure 8N). Similarly, presynaptic (but not postsynaptic) RNAi downregulating DNrx expression prevented DNlg1 clustering (Figure S7). Thus, presynaptic DNrx is required for effective accumulation of DNlg1 at a compartment adjacent to PSDs. However, the fact that the *dnrx* phenotype is clearly weaker than the *dnlg1* phenotype indicates that not all DNlg1 signaling and thus protein seems to be lost in the absence of presynaptic DNrx. Collectively, because *dnrx* phenotypes appear qualitatively similar but not of the same severity as *dnlg1* phenotypes, clustering of DNlg1 via presynaptic DNrx seems to promote DNlg1 signaling, but does not seem to be an absolute requirement for it.

DISCUSSION

Nlgs are generally considered to play an important role in the establishment of fully functional neuronal circuits (Varoqueaux et al., 2006; Hoon et al., 2009). Nlgs bind Nrxs (Ichtchenko et al., 1995; Südhof, 2008), and both proteins are sufficient to induce synapse formation in cultured cells (Scheiffele et al., 2000; Graf et al., 2004). Major issues, however, concerning the precise role of Nlgs for synapse formation, maturation, and maintenance have therefore remained open and are actively discussed (Südhof, 2008). These aspects include whether Nlgs can execute actual synaptogenic functions or are restricted to synapse maturation, maintenance, or both. To what extent functions of Nlgs can be reduced to retrograde signaling via Nrxs is another question.

Drosophila Nlg1 Functions in the Developmental Addition of Synaptic Boutons

Here, in an unbiased EMS mutagenesis screen, we identify a *Drosophila* Nlg family protein, DNlg1. Null mutations in *Drosophila dnlg1* dramatically reduced the number of synaptic boutons (Figure 1). Consistent with a reduction in terminal size, the number of the remaining synapses per NMJ was similarly reduced. Electrophysiological analysis suggested that the reduction in synapses provoked a similar reduction in the amount of neurotransmitter released per action potential. In contrast to findings in mice, where electrophysiological, but not structural, abnormalities were observed in *nlg* triple mutants (Varoqueaux et al., 2006), the functional defects at *Drosophila* NMJs seem to be largely a consequence of the structural defects.

Notably, DNlg1 is not required for the initial formation of synaptic terminals per se, because NMJs form on all muscles of *dnlg1* mutant animals, with an apparently normal timing (Figure S2). In addition, approximately 50% of the synapses are still present and largely functional, also at later stages. DNlg1, however, is required for effective addition of synaptic boutons during NMJ development and growth. We performed extended in vivo imaging of synaptic terminals at wild-type and mutant NMJs (Zito et al., 1999; Rasse et al., 2005; Schmid et al., 2008), finding that the *dnlg1* phenotype clearly reflects a genuine inability to effectively add new synaptic boutons to a synaptic terminal, but does not arise as a secondary deficit in the stability of previously assembled boutons (Figure 1). Thus, the inability to add new boutons, identified as the hallmark of this complementation group in the unbiased screen, leads to the reduction of NMJ size at the end of larval development. The reduction in bouton numbers also correlated with a reduction in the total number of synapses per NMJ. Establishment of a direct causal relation awaits further genetic dissection of DNlg1 signaling. Clearly, however, DNlg1 is not absolutely essential, because residual boutons still form. Thus, DNlg1 might be regarded more as a regulatory factor than an essential building block of synapses, consistent with its localization adjacent to, but not overlapping with, PSDs labeled by GluRs.

DNlg1 Functions in Postsynaptic Differentiation

Assembly of the postsynaptic apparatus did not take place for a significant fraction of boutons and individual synapses, whereas the accumulation of presynaptic markers was essentially normal. Again, we used live imaging to demonstrate a genuine postsynaptic assembly deficit, because boutons lacking SSR differentiation develop and continuously add presynaptic BRP-positive AZs without signs of presynaptic dedifferentiation (Figure 3). It thus appears that DNlg1 coordinates the formation of the postsynaptic compartment at the larval NMJ, including the proper localization of GluR clusters and the formation of the SSR and PSDs. We previously showed that a genetically induced lack of GluR complexes interferes with formation of the SSR (Schmid et al., 2006). Thus, an inability to target, transport, or maintain GluRs sufficiently (or some combination thereof) might be at the center of the postsynaptic differentiation or maturation deficits.

The links between bouton defects and individual AZ deficits remain to be addressed. Mutations in *dnlg1* affected NMJs both at the single-bouton level and at the single-synapse level, but they affected these synaptic structures only partially. On the other hand, increased DNlg1 levels were able to trigger molecular aspects of postsynaptic differentiation even at type II boutons, emphasizing the rate-limiting character DNlg1 can play for assembly processes in this system. The partial character of these phenotypes is not due to residual DNlg1 activities in our alleles because a deletion allele with the entire *dnlg1* open reading frame removed resulted in the very same phenotypes. Pathways operating in parallel, upstream, or both of DNlg1 and related differentiation processes need to be addressed in future analyses. Our electron microscopy analysis showed that planar appositions between presynaptic AZ membranes and postsynaptic membranes, a hallmark of synapse formation, still formed in bouton regions where the postsynaptic assembly largely failed (indicated by a lack of SSR). Thus, consistent with genetic analysis in mammals, at least some fundamental aspects of synapse formation—likely involving the deposition of specific cell adhesion proteins at both presynaptic and postsynaptic membrane—continue in *dnlg1* mutants.

Structure-Function Analysis of DNlg1: Relation to Neurexin Function

The prominent in vivo phenotype that we report for an Nlg family protein allowed the mechanistic analysis of this important gene family at the *Drosophila* NMJ. All evidence, particularly functional rescue analysis, conclusively demonstrated that DNlg1 operates in the postsynaptic muscle compartment. When overexpressed, DNlg1 lacking the cytoplasmic domain (DNlg1-GFP$^{\Delta cyto}$) displayed a drastic dominant-negative phenotype. Because DNlg1-GFP$^{\Delta cyto}$ was effectively targeted to the NMJ, it appears plausible that it still incorporates into DNlg1 signaling complexes but abrogates their functionality. Thus, apart from ectodomain-mediated interactions to proteins other than DNrx, the cytoplasmic domain seems also essential for the role of DNlg1 complexes in addition to that of presynaptic boutons. The cytoplasmic interactions of DNlg1 most likely consist of physical links to submembrane scaffold proteins. This is true, at least in part, for Nlg-2, which connects to the PSD proteins gephyrin and collybistin at GABAergic and glycinergic synapses (Poulopoulos et al., 2009). At vertebrate excitatory synapses, interactions similar to postsynaptic scaffolding proteins such as PSD-95 support Nlg function (Irie et al., 1997; Levinson et al., 2005). The fact that DNlg1-GFP$^{\Delta extra}$ (ectodomain deleted) is still localized to type I NMJ terminals and triggers ectopic clusters of postsynaptic proteins further underlines the role of the cytoplasmic domain in mediating protein-protein interactions. Thus, while future mechanistic analysis should also include expression of similar constructs under physiological expression levels, screening for interactions with the loss- and gain-of-function phenotypes is warranted.

Interaction with presynaptic Nrxs is thought to be of prime importance for Nlg function (Südhof, 2008). However, depending on the assay and context studied, results that conflict with this hypothesis are reported (Ko et al., 2009b). In preliminary cell aggregation and immoprecipitation experiments, we were unable to detect direct interaction between DNrx and DNlg1 (data not shown). It thus remains to be shown that DNlg1 interacts with DNrx directly. In principle, DNrx and DNlg1 could be part of larger complexes that might also comprise *Drosophila* homologs of an alternative postsynaptic Nrx receptor, called LRRTM2 (de Wit et al., 2009; Ko et al., 2009a). Irrespective of the exact nature of the protein-protein interactions, we here present evidence that presynaptic *Drosophila* Nrx promotes DNlg1 function, but is not an absolute prerequisite for it. First, while some aspects of the *dnlg1* phenotype are similar to *dnrx* mutant terminals (reduction of bouton numbers, ruffles in AZ, irregular receptor fields), they all are quantifiably less pronounced. Second, the most extreme phenotype (entire boutons lacking postsynaptic differentiation) was absent at *dnrx* terminals. Third, the severity of the *dnlg1* phenotype did not increase upon simultaneous elimination of DNrx, consistent with the idea that both proteins regulate a similar biological process or that DNrx functions are fully mediated via DNlg1.

Endogenous DNlg1 forms discrete clusters close to, but not identical with, PSD regions. In fact, loss of presynaptic DNrx severely reduced the numbers of DNlg1 clusters. DNrx and DNlg1 clusters often appear apposed at corresponding presynaptic and postsynaptic sites, perhaps defining a new synaptic "compartment." The DNlg1 ectodomain together with the transmembrane region seems to be sufficient for the assembly of DNlg1 clusters, while active signaling seems to depend on the cytoplasmic domain. Nrx binding might contribute to this ectodomain-mediated integration, because the dominant-negative effect of DNlg1 overexpression could be suppressed by either blocking DNrx binding by a point mutation or expressing it in a *dnrx* mutant background (Figure 8). Taken together, our data imply that presynaptic Nrx binding promotes accumulation of Nlg clusters at the postsynaptic membrane. Loss of this Nrx-binding activity weakens, but does not eliminate, Nlg signaling.

EXPERIMENTAL PROCEDURES

Genetics

The *dnlg1* alleles F1109, G998, H324, H453, H703, I960, K1132, and K1809 were isolated in an EMS mutagenesis screen (Aberle et al., 2002) employing CD8-GFP-Sh flies (Zito et al., 1999). The *dnlg1* excision alleles were generated by deleting the genomic DNA between two insertion elements carrying FRT sites (*dnlg1*$^{ex1.9}$ [PBacf00735 and PBacf00756], *dnlg1*$^{ex2.3}$ [PBacf00756 and PXPd00812], and *dnlg1*$^{ex3.1}$ [PBacf00735 and PXPd00812]). UAS-*fasII*, mef2-Gal4, and elav-Gal4 were kind gifts of C. Goodman. OK6-Gal4 has been described (Aberle et al., 2002). The UAS-*dnlg1*-IR RNAi lines (ID42616 and ID104209) were obtained from the VDRC stock center (Dietzl et al., 2007). Genetic analysis of *dnrx* was performed using the excision allele *dnrx*^{241} (Li et al., 2007). *dnrx*, *dnlg1* double mutants were generated by meiotic recombination and verified by PCR and complementation analysis. All deficiency lines were ordered from the Bloomington or Harvard stock centers. For wild-type control strains, *w*^{1118} or *w*^{1118};; CD8-GFP-Sh were used.

Cloning and Molecular Analysis of *dnlg1* and *dnrx*

The EMS-induced point mutations formed a complementation group and were mapped to *dnlg1* using available deficiencies, meiotic recombination, and single-nucleotide polymorphisms. Df(3R)Antp17, Df(3R)Dsx29, Df(3R)D7, Df(3R)D6, and Df(3R)dsx11 failed to complement the *dnlg1*^{I960} allele, whereas Df(3R)Antp1, Df(3R)Exel614, Df(3R)roe, and Df(3R)Scx4 did complement. The *dnlg1* alleles were sequenced on both strands (see Supplemental Experimental Procedures). A full-length *dnlg1* cDNA clone (RE29404) was obtained from DGRC (Stapleton et al., 2002). The *dnlg1* cDNA was used to synthesize three different digoxigenin-labeled sense and antisense probes (Roche) using T3 and T7 polymerases (Ambion). In situ hybridizations were performed according to standard protocols (Tautz and Pfeifle, 1989).

Full-length DNlg1-GFP was generated by insertion of EGFP between aa A865 and L866 (see Supplemental Experimental Procedures). The pUAST-*dnlg1*-GFP vector was used as a template to generate *dnlg1*-GFP$^{\Delta cyto}$ (aa 1–865, followed by EGFP) and *dnlg1*-GFP$^{\Delta extra}$ (aa 1–741 was deleted and replaced by a cassette containing a signal peptide from rat CD2 followed by 10 myc tags). DNrx-GFP was generated by PCR using cDNA clone LP14275 (Stapleton et al., 2002). EGFP was inserted between aa N1748 and T1749 (see Supplemental Experimental Procedures).

Site-directed mutagenesis was performed using the QuickChange XL kit (Stratagene). The D356R exchange corresponds to the mutation D271R in rat Nlg1 (Reissner et al., 2008). All DNlg1 constructs were first subcloned into the entry vector pENTR of the gateway cloning system (Invitrogen) and then transferred into the pUAST*attB* expression vector. DNlg1 transgenic fly strains were generated based on the φC31-mediated integration system using the landing site at the cytological position 68E (Bischof et al., 2007).

Antibody Production and Immunohistochemistry

For the DNlg1 antibody, a rabbit polyclonal serum was raised (Seqlab) against a synthetic peptide (C-QQFQPAPGRSITTNI) representing aa 1340–1354 of DNlg1. Wandering third-instar larvae were dissected in PBS and fixed for 15 min in 3.7% formaldehyde. Larval fillets were stained as described (Beuchle et al., 2007). Dilutions of primary antibodies used are as follows: rabbit anti-Ank2-XL 1:1000 (Koch et al., 2008), rabbit anti-DVGLUT (Mahr and Aberle,

2006), rabbit anti-GluRIIC and GluRIID 1:1000 (Qin et al., 2005), mouse anti-BRP 1:100 (Wagh et al., 2006), anti-HRP conjugated to Cy5 1:200 (Dianova), mouse anti-Syt 1:20 (clone 3H2), and mouse anti-Dlg (clone 4F3; kind gifts of C. Goodman). Fluorescently labeled secondary antibodies conjugated to Alexa 488, Alexa 568, or Alexa 647 (Invitrogen) were diluted 1:1000. Mounted larvae were examined using a LSM510 (Zeiss) confocal laser scanning microscope. DNlg1 signals were quantified by acquiring 16 bit confocal images (TCS SP5, Leica Mircosystems) of type Ib boutons (see Supplemental Experimental Procedures for details). For the quantification of GluRIID receptor field size, confocal image stacks (TCS SP5, Leica Microsystem) were analyzed using ImageJ and Bitplane Imaris 6.15 (see Supplemental Experimental Procedures).

Analysis of NMJs

The number of synaptic boutons (type Ib + Is) was quantified on dorsal muscles 1/9 in abdominal segments A3 of intact CD8-GFP-Sh third-instar larvae. The approximate muscle surface area was calculated by measuring the width and length of each fiber. Bouton density was defined as the number of boutons per synaptic branch length. Bouton diameter was determined for the largest bouton on muscles 1/9 by measuring the diameter crosswise followed by averaging of the two values.

For in vivo imaging, first-instar larvae were transferred into a drop of 70% glycerol/PBS and immobilized by an adequate coverslip. Larvae were transferred singly on yeasted fruit agar plates for recovery and imaging at the third-instar stage. Growing synaptic branches were distinguished from nongrowing branches by the addition of at least one bouton to a branch present at the LI stage. In vivo imaging of BRP-short-Strawberry (Schmid et al., 2008) was performed as described (Rasse et al., 2005).

Electrophysiology and Electron Microscopy

TEVC recordings were performed as previously described (Owald et al., 2010). All recordings were performed on muscle 6 of male third-instar larvae (segments A2 and A3) in HL3 (70 mM NaCl, 5 mM KCl, 20 mM $MgCl_2$, 10 mM $NaHCO_3$, 5 mM trehalose, 115 mM sucrose, 5 mM HEPES, and 1 mM or 0.5 mM $CaCl_2$ [pH 7.2]). For electron microscopy, conventional room temperature embedding was performed as described previously (Fouquet et al., 2009).

SUPPLEMENTAL INFORMATION

Supplemental Information for this article includes eight figures and Supplemental Experimental Procedures and can be found with this article online at doi:10.1016/j.neuron.2010.05.020.

ACKNOWLEDGMENTS

We thank Corey Goodman, David Featherstone, Nicholas Harden, the Bloomington Drosophila Stock Center, the VDRC Stock Center, the Harvard Exelixis Collection, the Developmental Studies Hybridoma Bank, and the *Drosophila* Genome Research Center for providing fly stocks and reagents. We would also like to thank Elke Naffin, Christine Quentin, Franziska Zehe, Anastasia Stawrakakis, and Madeleine Brünner for excellent technical assistance. We are grateful to Christian Klämbt, Bernd Goellner, David Featherstone, and Andrew Plested for discussions and critical comments on the manuscript. This work was supported by grants from the Deutsche Forschungsgemeinschaft to S.J.S. (Exc 257, SFB 665) and H.A. (Ab116/3-2).

Accepted: May 18, 2010
Published: June 9, 2010

REFERENCES

Aberle, H., Haghighi, A.P., Fetter, R.D., McCabe, B.D., Magalhães, T.R., and Goodman, C.S. (2002). wishful thinking encodes a BMP type II receptor that regulates synaptic growth in Drosophila. Neuron *33*, 545–558.

Araç, D., Boucard, A.A., Ozkan, E., Strop, P., Newell, E., Südhof, T.C., and Brunger, A.T. (2007). Structures of neuroligin-1 and the neuroligin-1/neurexin-1 beta complex reveal specific protein-protein and protein-Ca2+ interactions. Neuron *56*, 992–1003.

Atwood, H.L., Govind, C.K., and Wu, C.F. (1993). Differential ultrastructure of synaptic terminals on ventral longitudinal abdominal muscles in Drosophila larvae. J. Neurobiol. *24*, 1008–1024.

Beuchle, D., Schwarz, H., Langegger, M., Koch, I., and Aberle, H. (2007). Drosophila MICAL regulates myofilament organization and synaptic structure. Mech. Dev. *124*, 390–406.

Bischof, J., Maeda, R.K., Hediger, M., Karch, F., and Basler, K. (2007). An optimized transgenesis system for Drosophila using germ-line-specific phiC31 integrases. Proc. Natl. Acad. Sci. USA *104*, 3312–3317.

Biswas, S., Russell, R.J., Jackson, C.J., Vidovic, M., Ganeshina, O., Oakeshott, J.G., and Claudianos, C. (2008). Bridging the synaptic gap: neuroligins and neurexin I in Apis mellifera. PLoS ONE *3*, e3542.

Brand, A.H., and Perrimon, N. (1993). Targeted gene expression as a means of altering cell fates and generating dominant phenotypes. Development *118*, 401–415.

Chih, B., Engelman, H., and Scheiffele, P. (2005). Control of excitatory and inhibitory synapse formation by neuroligins. Science *307*, 1324–1328.

Chubykin, A.A., Atasoy, D., Etherton, M.R., Brose, N., Kavalali, E.T., Gibson, J.R., and Südhof, T.C. (2007). Activity-dependent validation of excitatory versus inhibitory synapses by neuroligin-1 versus neuroligin-2. Neuron *54*, 919–931.

Collins, C.A., and DiAntonio, A. (2007). Synaptic development: insights from Drosophila. Curr. Opin. Neurobiol. *17*, 35–42.

Dalva, M.B., McClelland, A.C., and Kayser, M.S. (2007). Cell adhesion molecules: signalling functions at the synapse. Nat. Rev. Neurosci. *8*, 206–220.

de Wit, J., Sylwestrak, E., O'Sullivan, M.L., Otto, S., Tiglio, K., Savas, J.N., Yates, J.R., 3rd, Comoletti, D., Taylor, P., and Ghosh, A. (2009). LRRTM2 interacts with Neurexin1 and regulates excitatory synapse formation. Neuron *64*, 799–806.

Dean, C., and Dresbach, T. (2006). Neuroligins and neurexins: linking cell adhesion, synapse formation and cognitive function. Trends Neurosci. *29*, 21–29.

Dietzl, G., Chen, D., Schnorrer, F., Su, K.C., Barinova, Y., Fellner, M., Gasser, B., Kinsey, K., Oppel, S., Scheiblauer, S., et al. (2007). A genome-wide transgenic RNAi library for conditional gene inactivation in Drosophila. Nature *448*, 151–156.

Dresbach, T., Neeb, A., Meyer, G., Gundelfinger, E.D., and Brose, N. (2004). Synaptic targeting of neuroligin is independent of neurexin and SAP90/PSD95 binding. Mol. Cell. Neurosci. *27*, 227–235.

Drysdale, R.; FlyBase Consortium. (2008). FlyBase : a database for the Drosophila research community. Methods Mol. Biol. *420*, 45–59.

Fabrichny, I.P., Leone, P., Sulzenbacher, G., Comoletti, D., Miller, M.T., Taylor, P., Bourne, Y., and Marchot, P. (2007). Structural analysis of the synaptic protein neuroligin and its beta-neurexin complex: determinants for folding and cell adhesion. Neuron *56*, 979–991.

Featherstone, D.E., Rushton, E., Rohrbough, J., Liebl, F., Karr, J., Sheng, Q., Rodesch, C.K., and Broadie, K. (2005). An essential Drosophila glutamate receptor subunit that functions in both central neuropil and neuromuscular junction. J. Neurosci. *25*, 3199–3208.

Fouquet, W., Owald, D., Wichmann, C., Mertel, S., Depner, H., Dyba, M., Hallermann, S., Kittel, R.J., Eimer, S., and Sigrist, S.J. (2009). Maturation of active zone assembly by Drosophila Bruchpilot. J. Cell Biol. *186*, 129–145.

Gilbert, M.M., and Auld, V.J. (2005). Evolution of clams (cholinesterase-like adhesion molecules): structure and function during development. Front. Biosci. *10*, 2177–2192.

Graf, E.R., Zhang, X., Jin, S.X., Linhoff, M.W., and Craig, A.M. (2004). Neurexins induce differentiation of GABA and glutamate postsynaptic specializations via neuroligins. Cell *119*, 1013–1026.

Grenningloh, G., Rehm, E.J., and Goodman, C.S. (1991). Genetic analysis of growth cone guidance in Drosophila: fasciclin II functions as a neuronal recognition molecule. Cell *67*, 45–57.

Griffith, L.C., and Budnik, V. (2006). Plasticity and second messengers during synapse development. Int. Rev. Neurobiol. *75*, 237–265.

Hoang, B., and Chiba, A. (2001). Single-cell analysis of Drosophila larval neuromuscular synapses. Dev. Biol. *229*, 55–70.

Hoon, M., Bauer, G., Fritschy, J.M., Moser, T., Falkenburger, B.H., and Varoqueaux, F. (2009). Neuroligin 2 controls the maturation of GABAergic synapses and information processing in the retina. J. Neurosci. *29*, 8039–8050.

Ichtchenko, K., Hata, Y., Nguyen, T., Ullrich, B., Missler, M., Moomaw, C., and Südhof, T.C. (1995). Neuroligin 1: a splice site-specific ligand for beta-neurexins. Cell *81*, 435–443.

Ichtchenko, K., Nguyen, T., and Südhof, T.C. (1996). Structures, alternative splicing, and neurexin binding of multiple neuroligins. J. Biol. Chem. *271*, 2676–2682.

Irie, M., Hata, Y., Takeuchi, M., Ichtchenko, K., Toyoda, A., Hirao, K., Takai, Y., Rosahl, T.W., and Südhof, T.C. (1997). Binding of neuroligins to PSD-95. Science *277*, 1511–1515.

Jamain, S., Quach, H., Betancur, C., Råstam, M., Colineaux, C., Gillberg, I.C., Soderstrom, H., Giros, B., Leboyer, M., Gillberg, C., and Bourgeron, T.; Paris Autism Research International Sibpair Study. (2003). Mutations of the X-linked genes encoding neuroligins NLGN3 and NLGN4 are associated with autism. Nat. Genet. *34*, 27–29.

Jia, X.X., Gorczyca, M., and Budnik, V. (1993). Ultrastructure of neuromuscular junctions in Drosophila: comparison of wild type and mutants with increased excitability. J. Neurobiol. *24*, 1025–1044.

Ko, J., Fuccillo, M.V., Malenka, R.C., and Südhof, T.C. (2009a). LRRTM2 functions as a neurexin ligand in promoting excitatory synapse formation. Neuron *64*, 791–798.

Ko, J., Zhang, C., Arac, D., Boucard, A.A., Brunger, A.T., and Südhof, T.C. (2009b). Neuroligin-1 performs neurexin-dependent and neurexin-independent functions in synapse validation. EMBO J. *28*, 3244–3255.

Koch, I., Schwarz, H., Beuchle, D., Goellner, B., Langegger, M., and Aberle, H. (2008). Drosophila ankyrin 2 is required for synaptic stability. Neuron *58*, 210–222.

Laumonnier, F., Bonnet-Brilhault, F., Gomot, M., Blanc, R., David, A., Moizard, M.P., Raynaud, M., Ronce, N., Lemonnier, E., Calvas, P., et al. (2004). X-linked mental retardation and autism are associated with a mutation in the NLGN4 gene, a member of the neuroligin family. Am. J. Hum. Genet. *74*, 552–557.

Levinson, J.N., Chéry, N., Huang, K., Wong, T.P., Gerrow, K., Kang, R., Prange, O., Wang, Y.T., and El-Husseini, A. (2005). Neuroligins mediate excitatory and inhibitory synapse formation: involvement of PSD-95 and neurexin-1beta in neuroligin-induced synaptic specificity. J. Biol. Chem. *280*, 17312–17319.

Li, J., Ashley, J., Budnik, V., and Bhat, M.A. (2007). Crucial role of Drosophila neurexin in proper active zone apposition to postsynaptic densities, synaptic growth, and synaptic transmission. Neuron *55*, 741–755.

Lisé, M.F., and El-Husseini, A. (2006). The neuroligin and neurexin families: from structure to function at the synapse. Cell. Mol. Life Sci. *63*, 1833–1849.

Lnenicka, G.A., and Mellon, D., Jr. (1983). Changes in electrical properties and quantal current during growth of identified muscle fibres in the crayfish. J. Physiol. *345*, 261–284.

Mahr, A., and Aberle, H. (2006). The expression pattern of the Drosophila vesicular glutamate transporter: a marker protein for motoneurons and glutamatergic centers in the brain. Gene Expr. Patterns *6*, 299–309.

Missler, M., Zhang, W., Rohlmann, A., Kattenstroth, G., Hammer, R.E., Gottmann, K., and Südhof, T.C. (2003). Alpha-neurexins couple Ca2+ channels to synaptic vesicle exocytosis. Nature *423*, 939–948.

Owald, D., Fouquet, W., Schmidt, M., Wichmann, C., Mertel, S., Depner, H., Christiansen, F., Zube, C., Quentin, C., Körner, J., et al. (2010). A Syd-1 homologue regulates pre- and postsynaptic maturation in Drosophila. J. Cell Biol. *188*, 565–579.

Poulopoulos, A., Aramuni, G., Meyer, G., Soykan, T., Hoon, M., Papadopoulos, T., Zhang, M., Paarmann, I., Fuchs, C., Harvey, K., et al. (2009). Neuroligin 2 drives postsynaptic assembly at perisomatic inhibitory synapses through gephyrin and collybistin. Neuron *63*, 628–642.

Qin, G., Schwarz, T., Kittel, R.J., Schmid, A., Rasse, T.M., Kappei, D., Ponimaskin, E., Heckmann, M., and Sigrist, S.J. (2005). Four different subunits are essential for expressing the synaptic glutamate receptor at neuromuscular junctions of Drosophila. J. Neurosci. *25*, 3209–3218.

Rasse, T.M., Fouquet, W., Schmid, A., Kittel, R.J., Mertel, S., Sigrist, C.B., Schmidt, M., Guzman, A., Merino, C., Qin, G., et al. (2005). Glutamate receptor dynamics organizing synapse formation in vivo. Nat. Neurosci. *8*, 898–905.

Reissner, C., Klose, M., Fairless, R., and Missler, M. (2008). Mutational analysis of the neurexin/neuroligin complex reveals essential and regulatory components. Proc. Natl. Acad. Sci. USA *105*, 15124–15129.

Sara, Y., Biederer, T., Atasoy, D., Chubykin, A., Mozhayeva, M.G., Südhof, T.C., and Kavalali, E.T. (2005). Selective capability of SynCAM and neuroligin for functional synapse assembly. J. Neurosci. *25*, 260–270.

Scheiffele, P., Fan, J., Choih, J., Fetter, R., and Serafini, T. (2000). Neuroligin expressed in nonneuronal cells triggers presynaptic development in contacting axons. Cell *101*, 657–669.

Schmid, A., Qin, G., Wichmann, C., Kittel, R.J., Mertel, S., Fouquet, W., Schmidt, M., Heckmann, M., and Sigrist, S.J. (2006). Non-NMDA-type glutamate receptors are essential for maturation but not for initial assembly of synapses at Drosophila neuromuscular junctions. J. Neurosci. *26*, 11267–11277.

Schmid, A., Hallermann, S., Kittel, R.J., Khorramshahi, O., Frölich, A.M., Quentin, C., Rasse, T.M., Mertel, S., Heckmann, M., and Sigrist, S.J. (2008). Activity-dependent site-specific changes of glutamate receptor composition in vivo. Nat. Neurosci. *11*, 659–666.

Song, J.Y., Ichtchenko, K., Südhof, T.C., and Brose, N. (1999). Neuroligin 1 is a postsynaptic cell-adhesion molecule of excitatory synapses. Proc. Natl. Acad. Sci. USA *96*, 1100–1105.

Stapleton, M., Liao, G., Brokstein, P., Hong, L., Carninci, P., Shiraki, T., Hayashizaki, Y., Champe, M., Pacleb, J., Wan, K., et al. (2002). The Drosophila gene collection: identification of putative full-length cDNAs for 70% of D. melanogaster genes. Genome Res. *12*, 1294–1300.

Südhof, T.C. (2008). Neuroligins and neurexins link synaptic function to cognitive disease. Nature *455*, 903–911.

Takeichi, M. (2007). The cadherin superfamily in neuronal connections and interactions. Nat. Rev. Neurosci. *8*, 11–20.

Tautz, D., and Pfeifle, C. (1989). A non-radioactive in situ hybridization method for the localization of specific RNAs in Drosophila embryos reveals translational control of the segmentation gene hunchback. Chromosoma *98*, 81–85.

Ushkaryov, Y.A., Petrenko, A.G., Geppert, M., and Südhof, T.C. (1992). Neurexins: synaptic cell surface proteins related to the alpha-latrotoxin receptor and laminin. Science *257*, 50–56.

Varoqueaux, F., Aramuni, G., Rawson, R.L., Mohrmann, R., Missler, M., Gottmann, K., Zhang, W., Südhof, T.C., and Brose, N. (2006). Neuroligins determine synapse maturation and function. Neuron *51*, 741–754.

Wagh, D.A., Rasse, T.M., Asan, E., Hofbauer, A., Schwenkert, I., Dürrbeck, H., Buchner, S., Dabauvalle, M.C., Schmidt, M., Qin, G., et al. (2006). Bruchpilot, a protein with homology to ELKS/CAST, is required for structural integrity and function of synaptic active zones in Drosophila. Neuron *49*, 833–844.

Washbourne, P., Dityatev, A., Scheiffele, P., Biederer, T., Weiner, J.A., Christopherson, K.S., and El-Husseini, A. (2004). Cell adhesion molecules in synapse formation. J. Neurosci. *24*, 9244–9249.

Wittenmayer, N., Körber, C., Liu, H., Kremer, T., Varoqueaux, F., Chapman, E.R., Brose, N., Kuner, T., and Dresbach, T. (2009). Postsynaptic Neuroligin1 regulates presynaptic maturation. Proc. Natl. Acad. Sci. USA *106*, 13564–13569.

Yamagata, M., Sanes, J.R., and Weiner, J.A. (2003). Synaptic adhesion molecules. Curr. Opin. Cell Biol. *15*, 621–632.

Zeng, X., Sun, M., Liu, L., Chen, F., Wei, L., and Xie, W. (2007). Neurexin-1 is required for synapse formation and larvae associative learning in Drosophila. FEBS Lett. *581*, 2509–2516.

Zito, K., Parnas, D., Fetter, R.D., Isacoff, E.Y., and Goodman, C.S. (1999). Watching a synapse grow: noninvasive confocal imaging of synaptic growth in Drosophila. Neuron *22*, 719–729.